Body-Centered Orthorhombic C_{16}: A Novel Topological Node-Line Semimetal

Jian-Tao Wang,[1,*] Hongming Weng,[1,2] Simin Nie,[1] Zhong Fang,[1,2] Yoshiyuki Kawazoe,[3] and Changfeng Chen[4]
[1]Beijing National Laboratory for Condensed Matter Physics, Institute of Physics, Chinese Academy of Sciences, Beijing 100190, China
[2]Collaborative Innovation Center of Quantum Matter, Beijing 100190, China
[3]New Industry Creation Hatchery Center, Tohoku University, Sendai 980-8579, Japan
[4]Department of Physics and High Pressure Science and Engineering Center, University of Nevada, Las Vegas, Nevada 89154, USA
(Received 5 February 2016; published 11 May 2016)

We identify by *ab initio* calculations a novel topological semimetal carbon phase in all-sp^2 bonding networks with a 16-atom body-centered orthorhombic unit cell, termed bco-C_{16}. Total-energy calculations show that bco-C_{16} is comparable to solid fcc-C_{60} in energetic stability, and phonon and molecular dynamics simulations confirm its dynamical stability. This all-sp^2 carbon allotrope can be regarded as a three-dimensional modification of graphite, and its simulated x-ray diffraction (XRD) pattern matches well a previously unexplained diffraction peak in measured XRD spectra of detonation and chimney soot, indicating its presence in the specimen. Electronic band structure calculations reveal that bco-C_{16} is a topological node-line semimetal with a single nodal ring. These findings establish a novel carbon phase with intriguing structural and electronic properties of fundamental significance and practical interest.

DOI: 10.1103/PhysRevLett.116.195501

Carbon is extremely versatile in its ability to form a rich variety of allotropes with a wide range of fascinating properties. It has long been known [1] that at ambient conditions graphite is the thermodynamically most stable carbon allotrope and that many structural transformations and modifications of carbon structures in various sp^2 and sp^3 bonding networks can be produced under various pressure and temperature conditions. Under high static pressure and high temperature conditions, graphite can be converted to cubic diamond [2–6] or twinned cubic diamond with $\{111\}$ hexagonal-diamond-like stacking faults [5,6]; meanwhile, under cold static compression, graphite can transform to diamondlike sp^3 carbon forms [7–14]. Additional cubic modifications of carbon have been produced during the heating of carbon soot or shock compression of polycrystalline graphite [15–18], which led to a proposed simple cubic carbon phase termed SC24 in $Pa\bar{3}$ symmetry [19] and a body-centered cubic carbon phase termed BC12 in $Ia\bar{3}d$ symmetry [20]. Moreover, a body-centered cubic carbon denoted BC8 is suggested to be the high-pressure modification of carbon derived from cubic diamond under pressure of ~1100 GPa [21].

The discovery of fullerenes [22], nanotubes [23], and graphene [24] has ignited tremendous interest in recent years to explore additional carbon structures in all-sp^2 bonding networks. Various hypothetical sp^2 carbon modifications [25–29] have been proposed, including the hexagonal $H6$ carbon [26], fcc-C_{20} [27], $ThSi_2$-type tetragonal bct4 carbon [28], and $SrSi_2$-type cubic K_4 carbon [29]; most of them, however, are dynamically unstable due to the presence of twisted π states [30]. Recent studies unveiled a new type of stable chiral framework structures comprising threefold, fourfold [30], and sixfold [31] helical chains in all-sp^2 bonding networks connected by ethene-type planar π conjugation. This discovery offers a new strategy for finding viable all-sp^2 carbon structures and helping solve yet unidentified carbon phases found in carbon blacks, carbon soot, and fullerene soot [32–38].

In this Letter, we identify by *ab initio* calculations a new all-sp^2 carbon allotrope in $Imma$ (D_{2h}^{28}) symmetry. This new carbon phase has a 16-atom body-centered orthorhombic unit cell, thus termed bco-C_{16}, and it can be regarded as a three-dimensional modification of graphite, consisting of benzene linear chains connected by ethene-type planar π conjugation. Total-energy calculations show that bco-C_{16} is comparable to solid fcc-C_{60} in energetic stability, and its dynamic stability is verified by phonon and molecular dynamics simulations. An excellent match of simulated and measured x-ray diffraction spectra indicates the presence of bco-C_{16} in detonation and chimney soot [36–38]. Electronic band structure calculations show that bco-C_{16} belongs to a new class of topological node-line semimetals, which exhibit novel electronic and transport properties [39–48].

The total-energy and phonon calculations were carried out using the density functional theory as implemented in the Vienna *ab initio* simulation package (VASP) [49]. The generalized gradient approximation (GGA) developed by Armiento-Mattsson (AM05) [50] was adopted for the exchange-correlation potential. The all-electron projector augmented wave (PAW) method [51] was adopted with $2s^2 2p^2$ treated as valence electrons. A plane wave basis set with a large energy cutoff of 800 eV was used. Forces on the ions were calculated using the Hellmann-Feynman theorem with a full geometry optimization. The energy

minimization was done over the atomic and electronic degrees of freedom using the conjugate gradient iterative technique. Convergence criteria employed for both the electronic self-consistent relaxation and the ionic relaxation were set to 10^{-8} eV and 0.01 eV/Å for energy and force, respectively. Electronic band structures were calculated using the Heyd-Scuseria-Ernzerhof hybrid functional (HSE06) [52]. Phonon calculations were performed using the phonopy package [53].

For three-dimensional chiral crystalline modification of carbon in all-sp^2 bonding networks, the structures with matching helical chains of complementary chirality are energetically more favorable than structures with helical chains of same chirality [30]. Based on this concept, we here build up a more favorable bco-C_{16} carbon structure with complementary chirality to correspond to the rh6 carbon with the same sixfold helices [31]. This new helical structure can be derived from an eight-atom $(2 \times 2 \times 1)$ hexagonal graphene lattice with one C-C bond breaking, obeying the Wells's approach [54]. As a result, the conjugated helical chains in bco-C_{16} carbon are connected to each other to form benzene linear chains [see Fig. 1(a)] in contrast to the benzene rings in a rh6 carbon [31].

We first characterize the crystal structure of bco-C_{16}, which has the lattice parameters $a = 7.8061$ Å, $b = 4.8772$ Å, $c = 3.2372$ Å with the carbon atoms occupying two nonequivalent atomic Wyckoff positions of 8i (0.3231, 0.25, 0.1258) and 8f (0.0885, 0.5, 0.5), denoted by C_1 and C_2, respectively, as shown in Fig. 1(a). This structure topologically corresponds to a two-dimensional $(2\sqrt{3} \times 2)$ graphenelike lattice with one-third double and two-thirds single carbon-carbon bonds. Therefore, it also can be regarded as a three-dimensional modification of graphite in *AA* stacking consisting of benzene linear chains

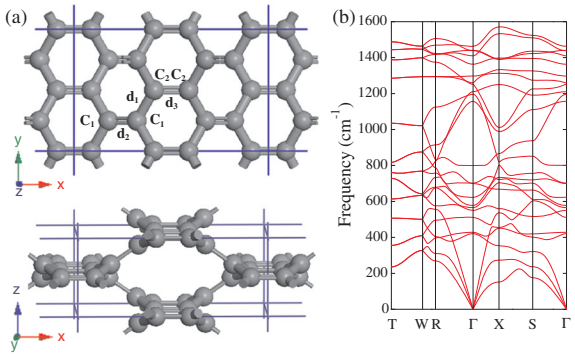

FIG. 1. Structure of bco-C_{16} and its phonon dispersion. (a) Top and side view of the all-sp^2 bco-C_{16} in *Imma* (D_{2h}^{28}) symmetry with one-third double (d_2, d_3) and two-thirds single (d_1) carbon-carbon bonds. It has a 16-atom body-centered orthorhombic structure with lattice parameters $a = 7.8061$ Å, $b = 4.8772$ Å, $c = 3.2372$ Å, occupying the 8*i* (0.3231, 0.25, 0.1258) and 8*f* (0.0885, 0.5, 0.5) Wyckoff positions, denoted by C_1 and C_2, respectively. (b) Calculated phonon dispersion curves of bco-C_{16} at zero pressure.

connected by ethene-type planar π conjugation. However, in contrast to the uniform bond length of 1.42 Å in graphite, there are three distinct carbon-carbon bond lengths, a longer bond of 1.459 Å (d_1) associated with a butadiene-type $C_1(sp^2) - C_2(sp^2)$ single bond and two shorter bonds of 1.396 Å (d_2) and 1.382 Å (d_3) associated with ethene-type planar $C_1(sp^2) = C_1(sp^2)$ and $C_2(sp^2) = C_2(sp^2)$ double bonds, respectively. There are also three different bond angles, $\angle C_1 = C_1 - C_2 = 123.19°$ out of the benzene rings, $\angle C_2 - C_1 - C_2 = 113.38°$ and $\angle C_1 - C_2 = C_2 = 118.23°$ in the benzene rings.

Figure 2 shows the calculated total energy versus volume per atom for bco-C_{16} compared to other carbon phases, including graphite, solid fcc-C_{60} fullerene [32], and the recently reported chiral framework structures cR6, cT8 [30], and rh6 carbon [31] in all-sp^2 bonding networks. Also shown for comparison are the results for diamond in an all-sp^3 bonding network and oC8 carbon in a mixed sp^2-sp^3 bonding network [14,20]. Key calculated data are listed in Table I. It is seen that the energetic stability of bco-C_{16} is comparable to that of fcc-C_{60} and oC8 carbon, and more favorable than those of the cR6, cT8, and rh6 carbon phases comprising three-, four-, sixfold helical carbon chains [30,31]. The equilibrium volume of bco-C_{16} is 7.7 Å^3 per atom, placing it between graphite and diamond. These energetic and volume data suggest possible synthesis of bco-C_{16} by compression of graphite. In fact, oC8 carbon, as a denser form of bco-C_{16}, has been found in the graphite-to-diamond phase conversion process [14], which is even more stable than graphite above 65 GPa (see Supplemental Material [55], Fig. S1).

We have performed a series of calculations to assess the mechanical stability of bco-C_{16}. We first calculated its elastic constants, and the obtained C_{11}, C_{22}, C_{33}, C_{44}, C_{55}, C_{66}, C_{12}, C_{13}, and C_{23} are 750, 877, 120, 80.5, 96.6, 336, 230, 141, and 37 GPa, respectively. These values meet the

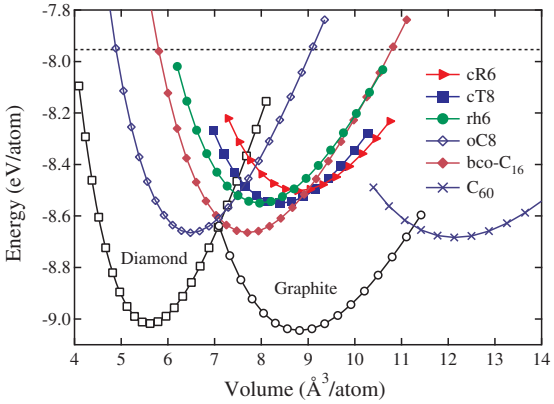

FIG. 2. Calculated energy versus volume per atom for bco-C_{16} compared to graphite, fcc-C_{60}, cR6, cT8, and rh6 carbon in all-sp^2, oC8 in mixed sp^2-sp^3, and diamond in all-sp^3 bonding networks. The dashed line indicates the energy level of carbyne chain.

TABLE I. Calculated equilibrium structural parameters (space group, volume V_0, lattice parameters a, b, and c, bond lengths d_{C-C}), total energy E_{tot}, bulk modulus B_0, and electronic band gap E_g for bco-C_{16} along with cR6, cT8, rh6, oC8 carbon, graphite, and diamond at zero pressure, compared to available experimental data [56].

Structure	Method	V_0(Å^3/atom)	a (Å)	b (Å)	c (Å)	d_{C-C} (Å)	E_{tot} (eV)	B_0 (GPa)	E_g (eV)
Diamond ($Fd\bar{3}m$)	AM05	5.60	3.552			1.538	−9.018	451	5.36
	Exp[56]	5.67	3.567			1.544		446	5.47
cR6 ($R\bar{3}m$)	AM05[30]	8.78	7.122		3.597	1.352, 1.490	−8.502	268	2.95
cT8 ($I4_1/amd$)	AM05[30]	8.40	5.937		3.808	1.351, 1.488	−8.551	283	2.41
rh6 ($R\bar{3}m$)	AM05[31]	7.96	6.902		3.470	1.359, 1.483	−8.550	299	0.47
oC8 ($Cmmm$)	AM05	6.49	7.789	2.500	2.665	1.346 ~ 1.632	−8.663	378	
bco-C_{16} ($Imma$)	AM05	7.70	7.806	4.877	3.237	1.382 ~ 1.459	−8.671	315	
Graphite ($P6_3/mmc$)	AM05	8.81	2.462		6.710	1.422	−9.045	280	
	Exp[56]	8.78	2.460		6.704	1.420		286	

criteria for mechanical stability given by C_{11}, C_{22}, C_{33}, C_{44}, C_{55}, and $C_{66} > 0$, $[C_{11} + C_{22} + C_{33} + 2(C_{12} + C_{13} + C_{23})] > 0$, $(C_{11} + C_{22}\text{-}2C_{12}) > 0$, $(C_{11} + C_{33}\text{-}2C_{13}) > 0$, and $(C_{22} + C_{33}\text{-}2C_{23}) > 0$ for orthorhombic phase [57]. We also calculated the phonon dispersion of bco-C_{16}, and the obtained results [see Fig. 1(b)] show no imaginary frequency in the entire Brillouin zone, confirming its dynamical stability. The highest phonon frequency is located at the X point with a value of ~1571 cm^{-1}, which is lower than but close to ~1600 cm^{-1} for graphite [58]. To further examine its thermal stability, *ab initio* molecular dynamics simulations were performed using a $2 \times 2 \times 2$ supercell. After being heated at room temperature (300 K) and then 1000 K for 3 ps with a time step of 1 fs, no structural changes occurred. These results show that bco-C_{16} is a viable carbon allotrope for experimental synthesis.

To establish the experimental connection of bco-C_{16}, we compare its simulated x-ray diffraction (XRD) spectra, along with those of graphite, diamond, rh6, cT8, cR6, fcc-C_{60}, to the experimental data from detonation soot of TNT and diesel oil [36] and chimney soot [37] as shown in Fig. 3. The measured XRD spectra reveal a considerable amount of amorphous carbon and provide clear evidence for several crystalline phases in the recovered specimen. The prominent peak around 26.5° is attributed to the graphite (002) diffraction, and the weak peak around 43.7°, matching that of the diamond (111) diffraction, indicates the presence of a small amount of cubic diamond. The most distinct feature of the measured XRD spectra is a strong peak at 30° that does not match any previously known carbon phases [36–38]; the high intensity and sharpness of this peak along with its consistent presence in different experiments suggest that a new crystalline carbon phase has been produced. Our simulated XRD results show that the main (101) diffraction peak of bco-C_{16} perfectly matches this previously unexplained peak. It is noted that the main peak of rh6 carbon is also close to 30° because it also comprises sixfold helices (or benzene rings) [31], but bco-C_{16} is energetically more stable with a substantial energy gain of 0.12 eV per carbon atom (see Fig. 2) due to its complementary chirality as mentioned above. These structural and energetic results suggest that bco-C_{16} is a likely candidate of the intriguing new carbon phase observed in the detonation and chimney soot [36–38].

Finally, we discuss the electronic properties of the new bco-C_{16} carbon. Our calculated results [Fig. 4(a)] show that the valence and conduction bands of bco-C_{16} exhibit linear

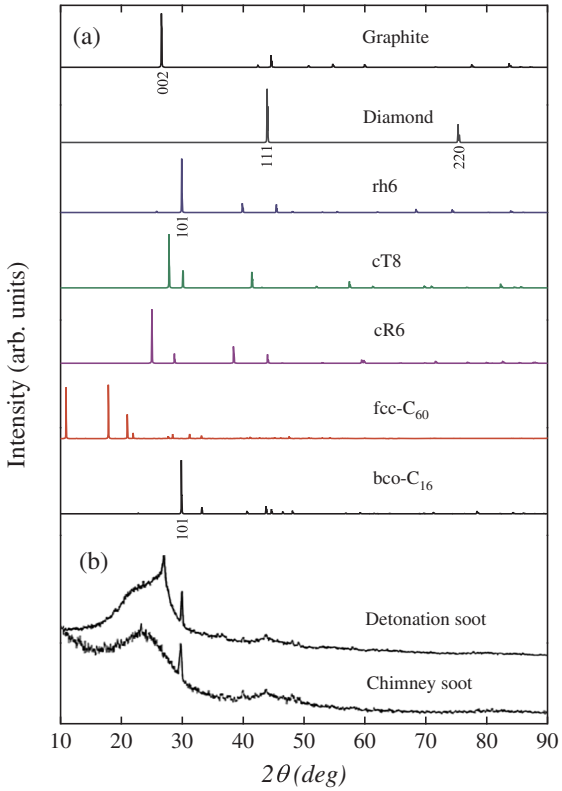

FIG. 3. X-ray diffraction (XRD) patterns. (a) Simulated XRD patterns for graphite, diamond, rh6, cT8, cR6, fcc-C_{60}, and bco-C_{16}. (b) Experimental XRD patterns for detonation soot of TNT and diesel oil [36] and chimney soot [37]. X-ray wavelength is 1.5406 Å with a copper source.

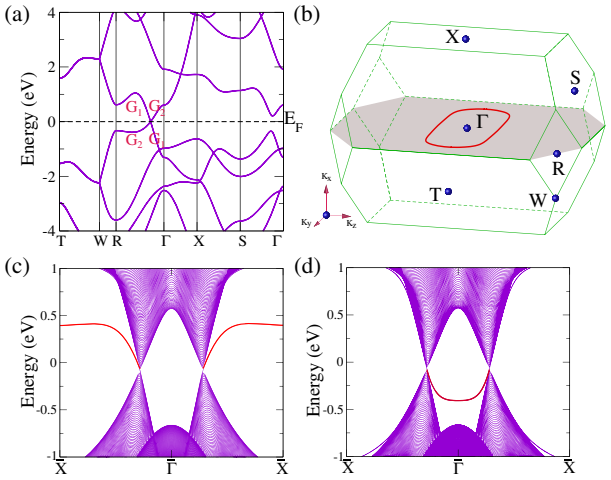

FIG. 4. Calculated bulk and surface band structures of bco-C_{16} at equilibrium lattice parameters. (a) The bulk band structure along several high-symmetry directions. G_1 and G_2 indicate the irreducible representation of the two crossing bands, respectively. (b) The Brillouin zone with several high-symmetry momenta indicated. The nodal ring (red circle), formed by the band crossing points, is in the shaded mirror plane. (c) and (d) show the surface states for different zigzaglike (c) and beardlike (d) terminations of the (100) surface. The surface flat band (red line) can be outside or inside the surface projected nodal ring.

dispersion near the Fermi energy and cross at the Fermi level, and further analysis of the band structure in the full Brillouin zone indicates that the band crossing points (or nodal points) of the valence and conduction bands in bco-C_{16} form a continuous nodal ring inside a mirror plane [the shaded region in Fig. 4(b)]. Moreover, the states near the crossing points around the nodal ring are formed by the inversion of the valence and conduction bands and protected by the coexistence of the time-reversal and inversion symmetry. These electronic properties characterize bco-C_{16} as a topological node-line semimetal [39–48]. When the nodal ring is projected onto the (100) surface, it produces topologically protected surface flat bands either inside or outside of the ring, depending on the termination of the surface, as shown in Figs. 4(c) and 4(d). These flat bands can be detected by photoelectron spectroscopy. The spin-orbit coupling (SOC) may open up a gap at the band crossing points, but the SOC in bco-C_{16}, estimated to be 0.74 meV, is negligibly weak at all but extremely low temperatures, thus not expected to alter the semimetal phase.

In summary, we have identified by means of *ab initio* calculations a new body-centered orthorhombic carbon structure in *Imma* (D_{2h}^{28}) symmetry in all-sp^2 bonding networks. The structural stability of this bco-C_{16} phase is verified by phonon mode analysis and *ab initio* molecular dynamics simulations. Electronic band structure calculations reveal that it is a topological node-line semimetal [39–42], and its low-energy bulk bands with linear dispersion and the flat surface bands are expected to produce unique transport properties and strong correlation physics [43–48]. Our findings should facilitate further exploration of this class of intriguing materials. The excellent match between the simulated and measured x-ray diffraction patterns suggest the presence of bco-C_{16} phase in detonation and chimney soot [36–38], which is mixed with other carbon phases. A major challenge is to find a route toward more effective synthesis of bco-C_{16} for more detailed studies. Similar challenges have been encountered and overcome in the early stages of research of other novel carbon phases, such as fullerenes, nanotubes, and graphene. The structural identification and characterization of bco-C_{16} reported in the present work provide crucial knowledge for fundamental understanding and further exploration of this new carbon allotrope [59].

This study was supported by the National Natural Science Foundation of China (Grants No. 11274356, No. 11274359, and No. 11422428) and the Strategic Priority Research Program of the Chinese Academy of Sciences (Grant No. XDB07000000). H. W., S. N., and Z. F. acknowledge the National 973 program of China (Grants No. 2011CBA00108 and No. 2013CB921700). C. F. C. acknowledges support by DOE under Cooperative Agreement No. DE-NA0001982.

*wjt@aphy.iphy.ac.cn

[1] E. D. Miller, D. C. Nesting, and J. V. Badding, Chem. Mater. **9**, 18 (1997).
[2] R. Clarke and C. Uher, Adv. Phys. **33**, 469 (1984).
[3] I. Irifune, A. Kurio, S. Sakamoto, T. Inoue, and H. Sumiya, Nature (London) **421**, 599 (2003).
[4] H. Sumiya and T. Irifune, J. Mater. Res. **22**, 2345 (2007).
[5] S. Scandolo, M. Bernasconi, G. L. Chiarotti, P. Focher, and E. Tosatti, Phys. Rev. Lett. **74**, 4015 (1995).
[6] P. Németh, L. A. J. Garvie, T. Aoki, N. Dubrovinskaia, L. Dubrovinsky, and P. R. Buseck, Nat. Commun. **5**, 5447 (2014).
[7] W. L. Mao, H. K. Mao, P. J. Eng, T. P. Trainor, M. Newville, C. C. Kao, D. L. Heinz, J. F. Shu, Y. Meng, and R. J. Hemley, Science **302**, 425 (2003).
[8] Q. Li, Y. M. Ma, A. R. Oganov, H. B. Wang, H. Wang, Y. Xu, T. Cui, H. K. Mao, and G. T. Zou, Phys. Rev. Lett. **102**, 175506 (2009).
[9] J. T. Wang, C. F. Chen, and Y. Kawazoe, Phys. Rev. Lett. **106**, 075501 (2011).
[10] M. Amsler, J. A. Flores-Livas, L. Lehtovaara, F. Balima, S. A. Ghasemi, D. Machon, S. Pailhes, A. Willand, D. Caliste, S. Botti, A. SanMiguel, S. Goedecker, and M. A. L. Marques, Phys. Rev. Lett. **108**, 065501 (2012).
[11] H. Y. Niu, X. Q. Chen, S. B. Wang, D. Z. Li, W. L. Mao, and Y. Y. Li, Phys. Rev. Lett. **108**, 135501 (2012).
[12] K. Umemoto, R. M. Wentzcovitch, S. Saito, and T. Miyake, Phys. Rev. Lett. **104**, 125504 (2010).

[13] Z. S. Zhao, F. Tian, X. Dong, Q. Li, Q. Q. Wang, H. Wang, X. Zhong, B. Xu, D. L. Yu, J. L. He, H. T. Wang, Y. M. Ma, and Y. J. Tian, J. Am. Chem. Soc. **134**, 12362 (2012).
[14] J. T. Wang, C. F. Chen, and Y. Kawazoe, J. Chem. Phys. **137**, 024502 (2012).
[15] M. Miki-Yoshida, L. Rendon, and M. Jose-Yacaman, Carbon **31**, 843 (1993).
[16] K. Yamada, Carbon **41**, 1309 (2003).
[17] K. Yamada, Y. Tanabe, and A. B. Sawaoka, Philos. Mag. A **80**, 1811 (2000).
[18] A. El Goresy, L. S. Dubrovinsky, P. Gillet, S. Mostefaoui, G. Graup, M. Drakopoulos, A. S. Simionovici, V. Swamy, and V. L. Masaitis, C. R. Geoscience **335**, 889 (2003).
[19] J. T. Wang, C. F. Chen, and Y. Kawazoe, Phys. Rev. B **85**, 214104 (2012).
[20] Z. Z. Li, C. S. Lian, J. Xu, L. F. Xu, J. T. Wang, and C. F. Chen, Phys. Rev. B **91**, 214106 (2015).
[21] M. D. Knudson, M. P. Desjarlais, and D. H. Dolan, Science **322**, 1822 (2008).
[22] H. W. Kroto, J. R. Heath, S. C. Obrien, R. F. Curl, and R. E. Smaliey, Nature (London) **318**, 162 (1985).
[23] S. Iijima, Nature (London) **354**, 56 (1991).
[24] K. S. Novoselov, A. K. Geim, S. V. Morozov, D. Jiang, Y. Zhang, S. V. Dubonos, I. V. Grigorieva, and A. A. Firsov, Science **306**, 666 (2004).
[25] G.-M. Rignanese and J.-C. Charlier, Phys. Rev. B **78**, 125415 (2008).
[26] A. Y. Liu, M. L. Cohen, K. C. Hass, and M. A. Tamor, Phys. Rev. B **43**, 6742 (1991).
[27] M. Côté, J. C. Grossman, M. L. Cohen, and S. G. Louie, Phys. Rev. B **58**, 664 (1998).
[28] R. Hoffmann, T. Hughbanks, M. Kertész, and P. H. Bird, J. Am. Chem. Soc. **105**, 4831 (1983).
[29] M. Itoh, M. Kotani, H. Naito, T. Sunada, Y. Kawazoe, and T. Adschiri, Phys. Rev. Lett. **102**, 055703 (2009).
[30] J. T. Wang, C. F. Chen, and Y. Kawazoe, Sci. Rep. **3**, 03077 (2013).
[31] J. T. Wang, C. F. Chen, E. G. Wang, and Y. Kawazoe, Sci. Rep. **4**, 04339 (2014).
[32] W. I. F. David, R. M. Ibberson, J. C. Matthewman, K. Prassides, T. J. S. Dennis, J. P. Hare, H. W. Kroto, R. Taylor, and D. R. M. Walton, Nature (London) **353**, 147 (1991).
[33] M. P. Ruiz, R. G. de Villoria, A. Millera, M. U. Alzueta, and R. Bilbao, Chem. Eng. J. (Lausanne) **127**, 1 (2007).
[34] W. Z. Zhu, D. E. Miser, W. G. Chan, and M. R. Hajaligol, Carbon **42**, 1463 (2004).
[35] A. E. Fals, V. G. Hadjiev, and F. C. R. Hernández, Mater. Chem. Phys. **140**, 651 (2013).
[36] P. W. Chen, F. L. Huang, and S. R. Yun, Carbon **41**, 2093 (2003).
[37] D. Pantea, S. Brochu, S. Thiboutot, G, Ampleman, and G. Scholz, Chemosphere **65**, 821 (2006).
[38] A. L. Vereshchagin and G. S. Yur'ev, Inorg. Mater. (USSR) **39**, 247 (2003).
[39] A. A. Burkov, M. D. Hook, and L. Balents, Phys. Rev. B **84**, 235126 (2011).
[40] M. Phillips and V. Aji, Phys. Rev. B **90**, 115111 (2014).
[41] H. Weng, Y. Liang, Q. Xu, R. Yu, Z. Fang, X. Dai, and Y. Kawazoe, Phys. Rev. B **92**, 045108 (2015).
[42] C. Fang, Y. Chen, H. Y. Kee, and L. Fu, Phys. Rev. B **92**, 081201 (2015).
[43] Y. Kim, B. J. Wieder, C. L. Kane, and A. M. Rappe, Phys. Rev. Lett. **115**, 036806 (2015).
[44] R. Yu, H. Weng, Z. Fang, X. Dai, and X. Hu, Phys. Rev. Lett. **115**, 036807 (2015).
[45] G. E. Volovik, Phys. Scr. **T164**, 014014 (2015).
[46] T. T. Heikkila and G. E. Volovik, arXiv:1504.05824.
[47] C. L. Zhang, Z. J. Yuan, G. Bian, S. Y. Xu, X. Zhang, M. Z. Hasan, and S. Jia, Phys. Rev. B **93**, 054520 (2016).
[48] G. Bian *et al.*, Nat. Commun. **7**, 10556 (2016).
[49] G. Kresse and J. Furthmüller, Phys. Rev. B **54**, 11169 (1996).
[50] R. Armiento and A. E. Mattsson, Phys. Rev. B **72**, 085108 (2005).
[51] P. E. Blöchl, Phys. Rev. B **50**, 17953 (1994).
[52] A. V. Krukau, O. A. Vydrov, A. F. Izmaylov, and G. E. Scuseria, J. Chem. Phys. **125**, 224106 (2006).
[53] A. Togo, F. Oba, and I. Tanaka, Phys. Rev. B **78**, 134106 (2008).
[54] A. F. Wells, Acta Crystallogr. **7**, 535 (1954).
[55] See Supplemental Material at http://link.aps.org/supplemental/10.1103/PhysRevLett.116.195501 to show the calculted enthalpy-pressure curves for bco-C_{16}, oC8, rh6, rh6-II, M-carbon, Z-carbon, fcc-C_{136} clathrate, and cubic diamond measured relative to the value for graphite.
[56] F. Occelli, P. Loubeyre, and R. Letoullec, Nat. Mater. **2**, 151 (2003).
[57] Z. J. Wu, E. J. Zhao, H. P. Xiang, X. F. Hao, X. J. Liu, and J. Meng, Phys. Rev. B **76**, 054115 (2007).
[58] J. Maultzsch, S. Reich, C. Thomsen, H. Requardt, and P. Ordejón, Phys. Rev. Lett. **92**, 075501 (2004).
[59] See Supplemental Material at http://link.aps.org/supplemental/10.1103/PhysRevLett.116.195501, which includes Refs. [55,60–65], for carbon clathrates.
[60] H. A. Calderon, I. Estrada-Guel, F. Alvarez-Ramirez, V. G. Hadjiev, and F. C. Robles-Hernandez, Carbon **102**, 288 (2016).
[61] J. P. Perdew, K. Burke, and M. Ernzerhof, Phys. Rev. Lett. **77**, 3865 (1996).
[62] J. T. Wang, C. F. Chen, D. S. Wang, H. Mizuseki, and Y. Kawazoe, J. Appl. Phys. **107**, 063507 (2010).
[63] J. T. Wang, C. F. Chen, and Y. Kawazoe, Phys. Rev. B **84**, 012102 (2011).
[64] A. San-Miguel and P. Toulemonde, High Press. Res. **25**, 159 (2005).
[65] N. Rey, A. Munoz, P. Rodríguez-Hernández, and A. San-Miguel, J. Phys. Condens. Matter **20**, 215218 (2008).